EXHIBIT K

Tapon et al., *Cell* 105: 345-355 (2001)

Cell, Vol. 105, 345–355, May 4, 2001, Copyright ©2001 by Cell Press

The *Drosophila* Tuberous Sclerosis Complex Gene Homologs Restrict Cell Growth and Cell Proliferation

Nicolas Tapon,[1] Naoto Ito,[2] Barry J. Dickson,[3] Jessica E. Treisman,[4] and Iswar K. Hariharan[1,5]
[1]Massachusetts General Hospital Cancer Center
Building 149, 13th Street
Charlestown, Massachusetts 02129
[2]Molecular Neurogenetics Unit
Building 149, 13th Street
Charlestown, Massachusetts 02129
[3]Research Institute of Molecular Pathology
Dr Bohr-Gasse 7
A-1030 Vienna
Austria
[4]Skirball Institute for Biomolecular Medicine
and Department of Cell Biology
New York University Medical Center
540 First Avenue
New York, New York 10016

Summary

The inherited human disease tuberous sclerosis, characterized by hamartomatous tumors, results from mutations in either *TSC1* or *TSC2*. We have characterized mutations in the *Drosophila Tsc1* and *Tsc2/gigas* genes. Inactivating mutations in either gene cause an identical phenotype characterized by enhanced growth and increased cell size with no change in ploidy. Overall, mutant cells spend less time in G1. Coexpression of both *Tsc1* and *Tsc2* restricts tissue growth and reduces cell size and cell proliferation. This phenotype is modulated by manipulations in cyclin levels. In postmitotic mutant cells, levels of Cyclin E and Cyclin A are elevated. This correlates with a tendency for these cells to reenter the cell cycle inappropriately as is observed in the human lesions.

Introduction

The tuberous sclerosis complex (TSC) (Gomez, 1988) is characterized by tumorous growths called hamartomas that arise in a wide variety of tissues including the brain, skin, heart, and kidneys. Other symptoms of TSC include mental retardation and epilepsy. A feature of TSC is the presence of giant cells in some lesions, e.g., giant cell astrocytomas.

Approximately a third of the cases are familial and display an autosomal dominant pattern of inheritance. Two-thirds are sporadic mutations. About half of all familial TSC cases are associated with mutations at the *TSC1* locus, while mutations at the *TSC2* locus account for the rest (Young and Povey, 1998). *TSC1* encodes a 1164 amino acid protein, hamartin, which contains a stretch of hydrophobic amino acids as well as two putative coiled-coil domains. The *TSC2* locus encodes a 1807 amino acid protein called tuberin which includes a small region with sequence similarity to the GTPase-activating protein (GAP) domain for the Rap1 GTPase.

The hamartin and tuberin proteins have been shown to interact physically with each other and appear to exist as a complex in vivo (Nellist et al., 1999; Plank et al., 1998). Thus, disrupting the function of either protein could disrupt the formation of the complex. Consistent with this notion, mutations in either gene result in the same clinical abnormalities. At present, little is known about what lies upstream or downstream of these proteins in a signaling pathway. A variety of different biochemical activities have been attributed to tuberin. The putative GAP domain has been shown to increase the intrinsic GTPase activity of both Rap1a and Rab5 in vitro (Wienecke et al., 1995; Xiao et al., 1997). Tuberin can also modulate the transcriptional activity of AP1 and several members of the steroid hormone receptor family (Henry et al., 1998; Tsuchiya et al., 1996). Hamartin has also been shown to interact with the actin binding protein ezrin (Lamb et al., 2000). The role of each of these functions in restricting cellular growth and proliferation is unclear.

Several studies have addressed the ability of the TSC genes to alter the growth and proliferation of mammalian cells. Transfection of hamartin into tissue culture cells slows cell proliferation as does increased expression of tuberin (Miloloza et al., 2000; Soucek et al., 1997). A study using antisense oligonucleotides concluded that tuberin negatively regulates the G1/S transition (Soucek et al., 1997). Mice lacking tuberin (Kobayashi et al., 1999; Onda et al., 1999) die as embryos and exhibit hypoplasia of the liver and poor development of other abdominal organs. Heterozygous mice develop cysts and slow growing tumors in a variety of tissues as they age. The Eker rat, a model for hereditary renal cancer, is an insertion in the *TSC2* locus (Kobayashi et al., 1995; Yeung et al., 1994). Thus, as in the human disease, loss of *TSC1* or *TSC2* can promote cell proliferation in a variety of situations.

Mutations in the *Drosophila TSC2* homolog, *gigas* (henceforth *Tsc2*) result in a dramatic increase in the growth of mutant tissue and a cell autonomous increase in cell size (Ferrus and Garcia-Bellido, 1976; Ito and Rubin, 1999). Examination of mutant cells using confocal microscopy led to the conclusion that mutant cells were polyploid with approximately ten times the DNA content of wild-type cells (Ito and Rubin, 1999). These cells seemed to have normal patterns of DNA replication but were apparently blocked from entering mitosis. It was postulated that cells in *Tsc2* mutant clones undergo normal growth and progress through rounds of DNA replication without intervening M-phases. As a consequence, they would become polyploid and larger than wild-type cells.

Here, we describe mutations in the *Drosophila TSC1* homolog (*Tsc1*). Our interpretation of the *Tsc1* mutant phenotype differed significantly from that described previously for *Tsc2* and caused us to reexamine the *Tsc2* mutant phenotype. We conclude that either *Tsc1* or *Tsc2* mutant cells are large but retain normal ploidy.

[5]Correspondence: hariharan@helix.mgh.harvard.edu

Mutant cells display no block in mitosis but spend less time in the G1 phase of the cell cycle. *Tsc1* and *Tsc2* mutations also induce inappropriate cell cycle entry in populations of cells that are normally quiescent. We demonstrate that the two genes function together to restrict growth and proliferation and that they interact with known regulators of these processes.

Results

Identification of Mutations in Genes that Restrict Growth and Proliferation

To identify genes that restrict growth and proliferation in vivo, we screened for mutations that result in an increased representation of mutant tissue at the expense of wild-type tissue. Following mutagenesis, homozygous clones of mutant tissue were generated in the eyes of heterozygous animals at high frequency using a FLP-recombinase expressed under the control of regulatory elements from the *eyeless* gene *(eyFLP)* (Newsome et al., 2000). Since the wild-type chromosome was marked with the dosage sensitive *mini-white* gene, we were able to compare the relative amounts of mutant tissue (phenotypically white, no copies of *mini-white*) with that of wild-type tissue (phenotypically red, two copies of *mini-white*). *eyFLP*-induced mitotic recombination was so efficient that very little heterozygous tissue (orange, one copy of *mini-white*) was seen. Competition throughout development between the mutant and wild-type clones determined the proportions of red and white tissue in the adult eye. We kept flies (~1% of those screened) where the representation of mutant over wild-type tissue was increased.

Our screens of the four major autosomal arms of *Drosophila* have identified more than 23 loci that result in an increased representation of mutant tissue (E. Buff, L. Edelmann, K. Moberg, N.T., and I.K.H., unpublished observations). One locus identified in the screen of the right arm of the third chromosome, was a lethal complementation group consisting of three members. The lethality of these mutations was uncovered by the deletion, *Df(3R)crb-F89-4*, which lacks the 95D07-D11 to 95F15 region. Ito and Rubin (1999) had identified a homolog of the *TSC1* gene (*Tsc1*) and mapped it to this region. Each mutant chromosome had a different single base change in the *Tsc1* gene that in each case resulted in a premature stop codon (Figure 1A). In each instance, this would result in the production of an extremely truncated protein lacking the coiled-coil domains which have been shown to be essential for the interaction of TSC1 with TSC2 in mammalian cells (Nellist et al., 1999). There is no obvious difference in the severity of the phenotype of the three alleles and each is lethal in trans to the others or when hemizygous. Thus, all three mutations are likely to represent null alleles of *Tsc1*.

Tsc1 Mutations Increase Cell Size and Organ Size

Eyes bearing clones of mutant *Tsc1* tissue were significantly larger than wild-type eyes with a substantial overrepresentation of mutant tissue over wild-type tissue (Figure 1B). The individual facets of the eye as well as the interommatidial bristles were significantly larger in the mutant portions of the eye (Figure 1B). Sections of

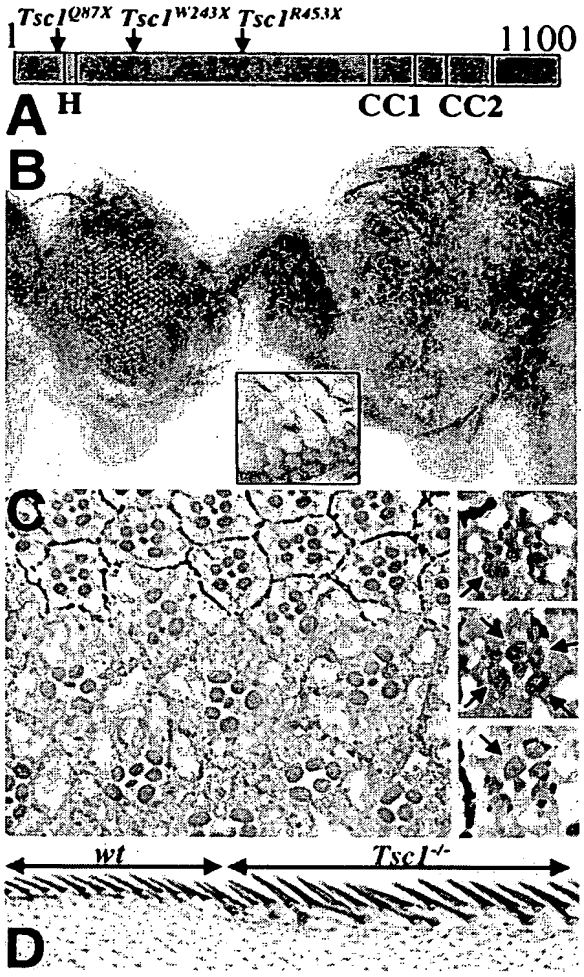

Figure 1. *Tsc1* Mutations Disrupt the *Drosophila TSC1* Homolog and Cause Increased Organ and Cell Size

(A) Positions of the premature stop codons resulting from the three *Tsc1* mutations (arrows). $Tsc1^{Q87X}$ changes codon 87 CAG (Gln) to TAG (stop); $Tsc1^{W243X}$ changes codon 243 TGG (Trp) to TGA (stop); and $Tsc1^{R453X}$ changes codon 453 CGA (Arg) to TGA (stop). The hydrophobic stretch (H) and coiled-coil domains (CC1 and CC2) are shown.

(B) Adult eyes mosaic for the parent chromosome bearing the FRT 82B element (left) and the $Tsc1^{Q87X}$ allele (right). Mutant clones are white and wild-type twin spots are red. FLP-induced mitotic recombination occurs in the eye disc as well as in the antennal disc, leading to enlarged eyes and head tissue in the mutant. The inset shows a clonal boundary at higher magnification. Mutant facets (white) are enlarged. Genotypes: *y w eyFLP; FRT82B/FRT82B P[mini-w, arm-lacZ]* (left); *y w eyFLP; FRT82B* $Tsc1^{Q87X}$ */FRT82B P[mini-w, arm-lacZ]* (right).

(C) Adult retinal section through a mosaic eye. Mutant tissue lacks the *white* pigment. *Tsc1* mutant cells are enlarged and have larger rhabdomeres. Genotype: *y w, eyFLP; FRT82B* $Tsc1^{Q87X}$ */FRT82B P[mini-w]*. Insets on the right show individual ommatidia of mixed genotypes at higher magnification. Rhabdomeres of outer photoreceptor cells (R1-6) of mutant genotype, which lack pigment granules, are arrowed. Wild-type rhabdomeres contain pigment granules. In wild-type ommatidia, the central R7 rhabdomere is smaller than those of R1-6 and its pigment cannot be observed in all sections. Genotype: *y w, eyFLP; FRT82B* $Tsc1^{Q87X}$ */FRT82B P[w]*.

(D) Enlarged bristles on the anterior wing margin in a *Tsc1* mutant clone (marked with *yellow*) compared with adjacent bristles of normal size. Genotype: *y w hsFLP; FRT82B* $Tsc1^{W243X}$*/ FRT82B P[πMyc] P[w, y]*.

the adult retina revealed that mutant ommatidia were larger than adjacent wild-type ommatidia (Figure 1C). The cell bodies of individual *Tsc1* cells were enlarged, as were the rhabdomeres in the photoreceptor cells. In ommatidia of mixed genotype the larger rhabdomeres were always mutant, indicating that the requirement for *Tsc* function is cell autonomous (Figure 1C). In addition to their increased size, mutant ommatidia occasionally had missing or extra photoreceptor cells, suggesting a defect in either photoreceptor specification or differentiation. Ommatidial misrotations were also observed near clonal boundaries, which might be a consequence of the juxtaposition of wild-type cells with larger mutant cells. Clones of *Tsc1* mutant tissue generated in the wing (Figure 1D) or the wing blade (data not shown) also displayed an enlarged cell phenotype. Thus, *Tsc1* functions as a negative regulator of cell size in a number of tissues. Moreover, the large cell phenotype of *Tsc1* mutants is similar to that described for mutations in the *Tsc2* gene (Ferrus and Garcia-Bellido, 1976; Ito and Rubin, 1999).

We examined the pattern of expression of *Tsc1* RNA by in situ hybridization (data not shown). *Tsc1* RNA of maternal origin is present at high levels in early embryos and is expressed uniformly later in embryogenesis. During the third larval instar, *Tsc1* RNA is expressed uniformly in all imaginal discs. An antibody to Tsc2 shows mottled cytoplasmic staining (Figures 2F and 2G).

Loss of *Tsc1* or *Tsc2* Increases Cell Growth

To determine the stage of development when abnormalities in cell and tissue size become apparent, we dissected eye imaginal discs from third instar larvae and pupae. Imaginal discs containing clones of tissue that are mutant for either *Tsc2* (Ito and Rubin, 1999) or *Tsc1* (Figure 2I) are significantly larger than wild-type imaginal discs (Figure 2H), indicating that *Tsc2* and *Tsc1* have a role in restricting imaginal disc growth.

In the eye-imaginal discs of third instar larvae (Figures 2A–2C), *Tsc1* mutant cells, outlined with phalloidin, were larger than adjacent wild-type cells. This difference in size became even more evident in the pupal retina where the mutant cells had clearly outgrown wild-type cells (Figures 2D and 2E). The nuclei of mutant cells, when visualized by staining with an antibody to the neuronal-specific nuclear protein ELAV (Robinow and White, 1991) (Figures 2B and 2C), were larger than those of adjacent wild-type cells. However, staining with DNA dyes such as propidium iodide or DAPI revealed that they have a more diffuse DNA staining pattern than their wild-type neighbors (data not shown). Thus, while the nuclei are larger, it was unclear whether these enlarged nuclei had increased amounts of DNA.

Mutant Cells Have Normal Ploidy and Enter S Phase Inappropriately

Cells were dissociated from the posterior portions of eye-imaginal discs cut along the morphogenetic furrow and their DNA content was examined by flow cytometry. A green fluorescent protein (GFP) marker on the wild-type chromosome allowed us to distinguish wild-type cells (GFP+) from mutant cells (GFP−). The *Tsc1* mutant cells were larger than wild-type cells as measured by forward scatter (Figure 2P). However, the mutant cells clearly fell into 2C and 4C populations as measured by the absorbance of the intercalating dye Hoechst 33342 and thus appeared to have a normal DNA content (Figure 2P). This result was surprising since it had previously been concluded that *Tsc2* mutant cells were highly polyploid (Ito and Rubin, 1999). We therefore analyzed the DNA content of cells from *Tsc2* imaginal discs and found that they also had increased size and a normal DNA content (Figure 2Q). Ito and Rubin (1999) had estimated the DNA content from confocal images after staining with a DNA dye. High levels of background staining may have led to the erroneous conclusion.

Cell cycles in the eye imaginal disc are developmentally regulated. During the growth of the eye disc in the first and second larval instars, cells proliferate asynchronously. During the third larval instar, the morphogenetic furrow moves from the posterior to the anterior end of the disc, bringing about a G1 cell cycle arrest and the onset of differentiation. Cells anterior to the furrow cycle asynchronously, while those posterior to the furrow undergo a single additional cell cycle, the second mitotic wave. Posterior to the second mitotic wave, cells exit from the cell cycle and undergo terminal differentiation.

S phases, visualized by BrdU incorporation, occur normally in the asynchronously dividing cells anterior to the morphogenetic furrow as well as in cells undergoing the second mitotic wave in both *Tsc2* and *Tsc1* mutant tissue (Figures 2J–2L). This is consistent with previous observations of *Tsc2* (Ito and Rubin, 1999). However, additional BrdU incorporation occurred posterior to the second mitotic wave in clones of either *Tsc2* or *Tsc1* mutant tissue. This additional incorporation was not easy to observe using the short labeling times used by Ito and Rubin (1999). BrdU incorporation in this region was restricted to the mutant clones. Thus, lack of *Tsc1* or *Tsc2* allows cells to enter S phase in regions where they are normally quiescent, indicating that *Tsc1* and *Tsc2* function is required for cells to exit normally from the cell cycle.

We used the anti-phos H3 antibody (Hendzel et al., 1997) to visualize mitotic nuclei (Figures 2M–2O). Both the first and second mitotic waves occurred normally in *Tsc1* or *Tsc2* mutant clones, with no delay when compared to adjacent wild-type cells. Moreover, additional mitoses are observed in mutant clones posterior to the second mitotic wave. Thus, cells that enter S phase appear to proceed through the remainder of the cycle with no evidence of a block in G2. When dissociated cells from the posterior portion of eye discs were analyzed, mutant populations had an increased proportion of cells in S phase (cycling cells) with no evidence of either a G2 block or polyploidy (Figures 2P and 2Q). Analysis of 45 hr pupal eye discs also confirmed normal ploidy at later stages of development (not shown).

In summary, *Tsc1* or *Tsc2* mutant cells are larger and consist of populations with a 2C or 4C DNA content. Moreover, in *Tsc2* or *Tsc1* mutant clones, ectopic S phases and mitoses are also observed at a stage when cells are normally mitotically quiescent. These results contradict the findings described in a publication (Ito and Rubin, 1999) where one of us (N.I.) was an author. Both authors of that study are now in complete agree-

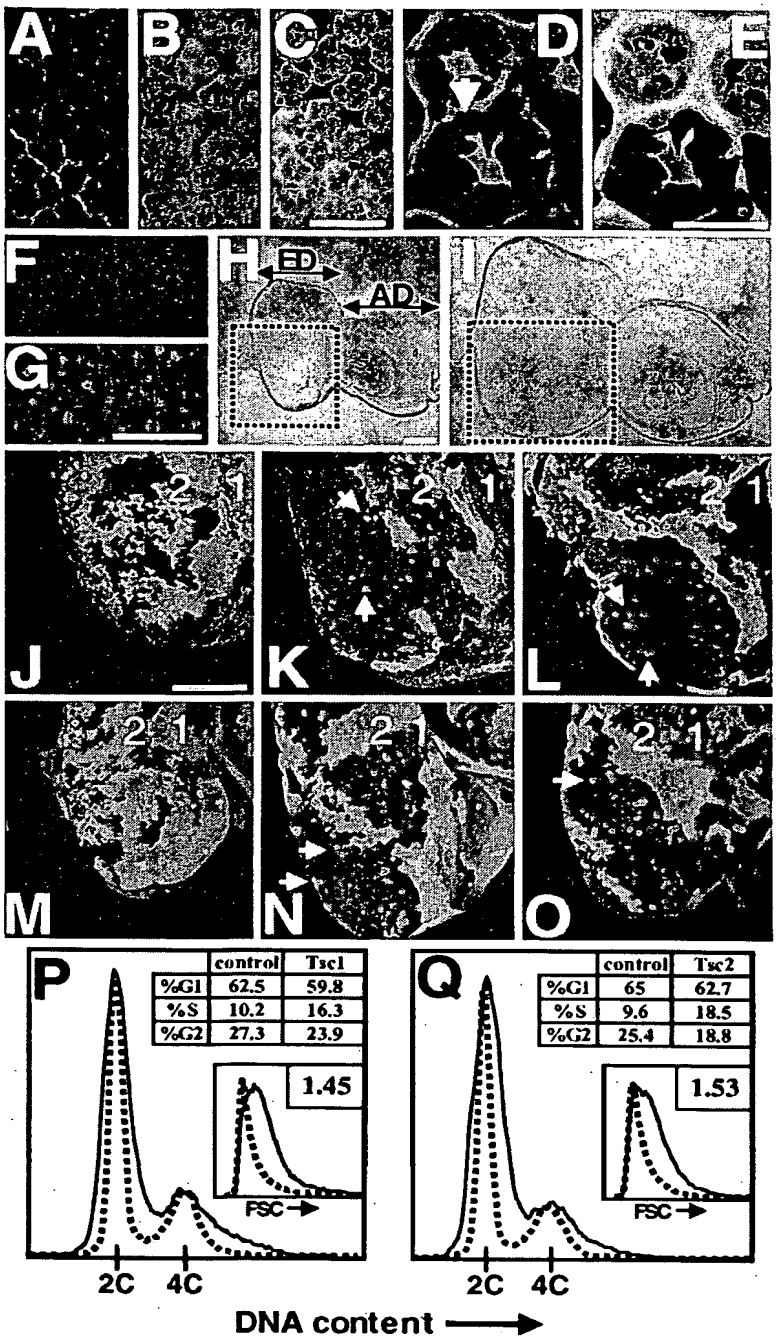

Figure 2. Cell Size and Cell Cycle Phenotypes of *Tsc1* and *Tsc2* Mutant Clones in Developing Eye Imaginal Discs

(A–C and F–O) Eye-imaginal discs from third instar larvae. Anterior is to the right.

(D and E) Eye imaginal disc from pupae (48 hr APF at 25°C).

(A–C) Increased cell and nuclear size in *Tsc1* mutant clones. (A) shows cells outlined with phalloidin (red). (B) shows photoreceptor nuclei stained with anti-ELAV (green). (C) is a merge of (A) and (B) and staining with anti-β-galactosidase (purple). Mutant cells in (C) fail to stain with anti-β-galactosidase. Scale bar = 25 μm.

(D and E) Increased size of mutant cells in the pupal retina. In (D) and (E), cells are outlined with phalloidin (red). Mutant cells fail to stain with anti-β-galactosidase (green). The arrow points to a small wild-type cell adjacent to larger mutant cells. Scale bar = 10 μm.

(F and G) Cytoplasmic localization of Tsc2 protein. In cells posterior to the morphogenetic furrow focused at the level of the basal nuclei, anti-Tsc2 (red) detects mottled cytoplasmic staining (F). Nuclei stained with DAPI (blue) are also shown in (G). Scale bar = 20 μm.

(H and I) Phase contrast images of eye-imaginal discs containing either wild-type (H) or *Tsc1*^{Q87X} clones (I). Scale bar = 50 μm. (ED refers to eye disc; AD to antennal disc). Regions corresponding to those boxed are shown in the fluorescent images (J–O).

(J–L) BrdU incorporation (red) showing S phases in third instar larval discs with clones of the parent chromosome (J), *Tsc1* (K), and *Tsc2* (L). Clones fail to stain with anti-β-galactosidase (green). "1" and "2" refer to the two waves of S phases. Both first and second waves were normal in *Tsc1* and *Tsc2* mutant clones. Ectopic S phases observed in the mutant clones are arrowed. Scale bar for J–O = 50 μm.

(M–O) Mitoses are visualized with the anti-phos H3 antibody (red) in third instar larval discs with clones of the parent chromosome (M), *Tsc1* (N) and *Tsc2* (O). Clones fail to stain with anti-β-galactosidase (green). "1" and "2" refer to the two waves of mitoses. Additional mitoses posterior to the second wave are arrowed.

(P and Q) Cells dissociated from posterior portions of third instar eye discs cut along the morphogenetic furrow examined by flow cytometry for DNA content and forward scatter (insets). Control (GFP+) populations—dashed line; mutant (GFP−) populations—solid lines. Relative increase in FSC of mutant cells for this experiment is included in the inset.

ment with the interpretation of the phenotype presented in this paper (G. Rubin, personal communication; see also Erratum, this issue of *Cell*).

Tsc1 or *Tsc2* Mutant Cells Spend Less Time in G1

To quantify the cycling properties of mutant cells, clones of *Tsc1* or *Tsc2* mutant cells were generated at high frequency in the third instar wing imaginal disc, and examined by flow cytometry (Neufeld et al., 1998). Wild-type (GFP +) cells were compared to (GFP−) mutant cells. Mutations in either *Tsc1* or *Tsc2* resulted in a significant increase in cell size over wild-type controls, as measured by an increase in forward scatter (Figures 3B and 3E). As in eye discs, both *Tsc1* and *Tsc2* mutant cells had a normal DNA content as assessed by staining with Hoechst 33342 and were not polyploid (Figures 3A and 3D). The 2C and 4C populations were also gated separately and displayed an identical shift in cell size

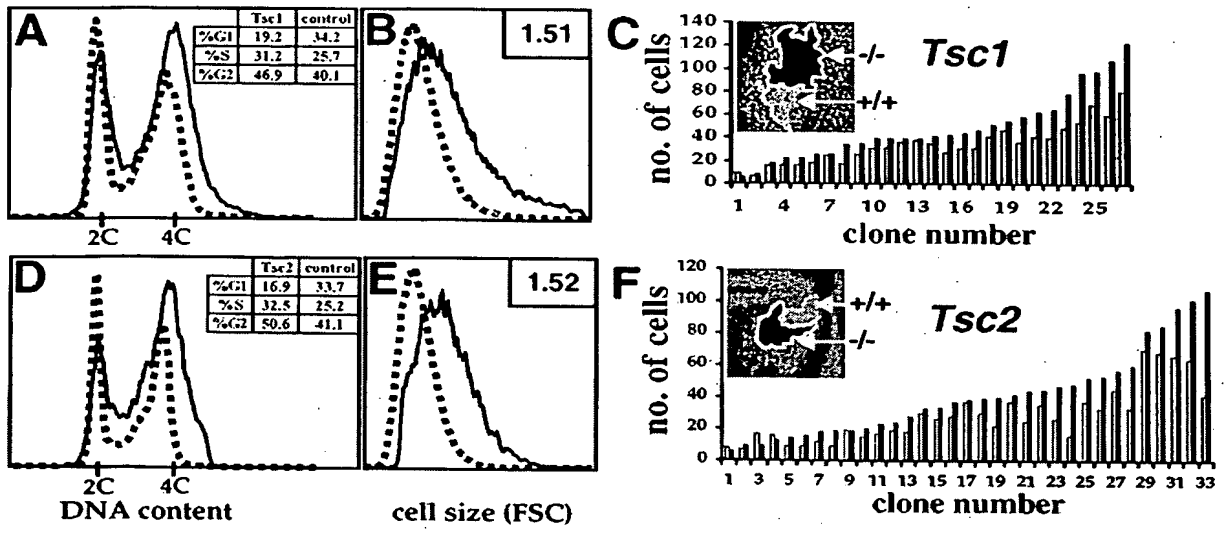

Figure 3. Increased Cell Size, Normal Ploidy and Cell Cycle Alterations in *Tsc1* and *Tsc2* Mutant Clones in the Third Instar Wing Disc

(A, B, D, and E) DNA content (A and D) and cell size (B and E) as assessed by flow cytometry for *Tsc1* (A and B) and *Tsc2* (D and E) cells. Control (GFP+) populations (dashed line) and mutant (GFP−) populations (solid line) are shown. Mean increase in FSC in mutant populations are indicated in the insets in B and E. Paired student's t tests indicated statistically significant increases in FSC for mutant over wild-type cells in data collected from three independent experiments for each genotype ($p = 0.0004$ for *Tsc1* and $p = 0.0047$ for *Tsc2*).

(C and F) Cell numbers in the mutant clone (black) and wild-type twin spot (gray) of individual clone pairs generated from the same recombination event ordered in increasing mutant clone size. ([C], *Tsc1*; [F], *Tsc2*). Insets show examples of clone/twin-spot pairs showing increased size of the mutant clone compared to the twin-spot. Clone and twin spot areas were also measured using the histogram function of Adobe Photoshop. Using a paired student's t test, the areas of mutant clones were found to be significantly larger than their twin spot pairs ($p = 0.0001$ for *Tsc1* and $p = 0.0004$ for *Tsc2*). For clone-twin spot pairs, mean increase in size was 2.0 for *Tsc1* and 2.2 for *Tsc2*.

(not shown). Thus, mutations in *Tsc1* or *Tsc2* result in an increase in cell size that is manifest at all stages of the cell cycle. Moreover, *Tsc1* and *Tsc2* mutant cells are underrepresented in the G1 fraction when compared to control populations. Instead, they are overrepresented in S and G2 fractions (Figures 3A and 3D).

We estimated the division times of mutant and wild-type cells by counting the number of cells in the mutant clone and its wild-type "twin spot" after a fixed time interval. The mutant clones are typically larger than the wild-type twin spot due to increased growth in the mutant clone (Figures 3C and 3F). Cell counts showed a small reduction in the division time (10%–15%) in the mutants when compared to control cells (see Experimental Procedures). Taken together with the altered phasing of the cell cycle, mutations in *Tsc1* and *Tsc2* appear to shorten G1 by almost 50%. There are small (6%–14%) increases in the length of the S and G2 phases.

Tsc1 and *Tsc2* Function Together to Restrict Growth and Proliferation

We generated fly stocks that expressed either *Tsc1* or *Tsc2* or both genes under the control of GAL4-responsive UAS elements and targeted their expression to the proliferating cells in the developing eye using the *ey-GAL4* driver line (Figures 4A–4D). While overexpression of either *Tsc1* or *Tsc2* alone had no effect, overexpression of *Tsc1* and *Tsc2* together resulted in a much smaller eye (Figure 4D). Coexpression of the baculovirus caspase inhibitor p35 did not alter this phenotype (data not shown), indicating that the phenotype did not result from increased cell death. Coexpressing *Tsc1* and *Tsc2* posterior to the morphogenetic furrow in the developing eye using the *GMR-GAL4* driver reduced the growth of postmitotic cells (data not shown). Thus, the two Tsc proteins function together to restrict tissue growth.

As in the eye, coexpression of both genes in the posterior compartment of the wing reduced its size (Figures 4E–4L). Since each cell in the adult wing secretes a single hair, we can infer cell numbers from the number of hairs. We counted the number of hairs in a small rectangular region of fixed size and location in the posterior compartment and compared it with a region of identical size in the anterior compartment (Figures 4I–4L; Table 1). The cell density in the posterior compartment was ~60% higher than in control wings, indicating a 1.6-fold reduction in cell size. Furthermore, the total area of the posterior compartment of the wing was reduced by approximately 2-fold. The inferred cell number in the posterior compartment was reduced by 27%. Thus, the reduction in compartment size is due to both a reduction in cell size and a reduction in cell number. Neither transgene on its own affected cell or compartment size.

To examine the effect of Tsc overexpression on cycling cells in the wing imaginal disc, we generated clones of GFP-marked cells that overexpress both *Tsc1* and *Tsc2* (Neufeld et al., 1998) and compared them to wild-type GFP-negative cells growing in the same disc (Figures 4M and 4N). Coexpression of *Tsc1* and *Tsc2* causes a reduction in the size of cycling cells. Cells overexpressing both *Tsc1* and *Tsc2* also displayed a relative

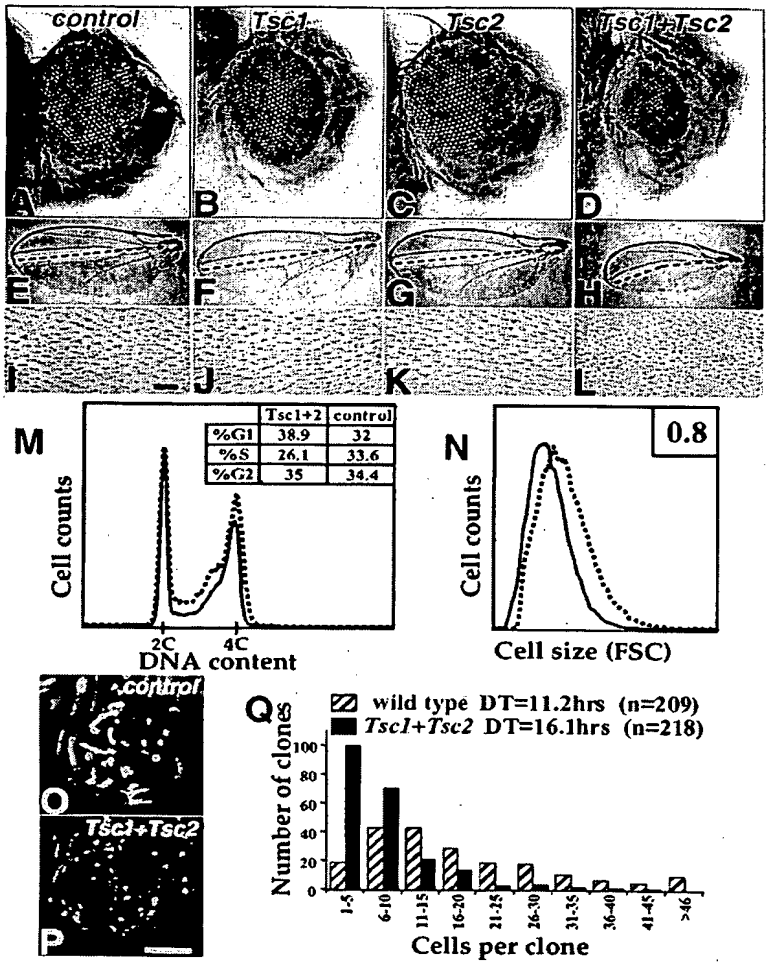

Figure 4. Overexpression of *Tsc1* and *Tsc2* Reduces Organ and Cell Size and Slows Cell Proliferation

(A–D) Adult eyes of flies expressing transgenes under the control of *eyGAL4*. Genotypes are *eyGAL4/+; +* (A); *eyGAL4/+; UAS-Tsc1/+* (B); *eyGAL4/+; UAS-Tsc2/+* (C); and *eyGAL4/+; UAS-Tsc1 UAS-Tsc2/+* (D).

(E–H) Adult wings of flies expressing transgenes under the control of *enGAL4*. Genotypes are *enGAL4/+; +* (E); *enGAL4/+; UAS-Tsc1/+* (F); *enGAL4/+; UAS-Tsc2/+* (G); and *enGAL4/+; UAS-Tsc1 UAS-Tsc2/+* (H). The dashed line indicates the A-P compartment boundary.

(I–L) High magnification images of a region from the posterior compartment of wings shown in (E–H). Scale bar = 25 μm.

(M and N) DNA content (M) and cell size (N) as assessed by flow cytometry for cells overexpressing both *Tsc1* and *Tsc2*. The distributions of control (GFP−) populations (dashed line) and double transgenic (GFP+) populations (solid line) are shown. Mean FSC in *Tsc1* + *Tsc2* overexpressing populations compared to control is indicated in the inset in (N). A paired student's t test using the results of three independent experiments indicated that the reduction in FSC was significant ($p = 0.0062$).

(O and P) FLP-out clones expressing either GFP alone (O) or GFP, *Tsc1*, and *Tsc2* (P) photographed 48 hr after induction by a 15 min heat shock. Scale bar = 100 μm.

(Q) Distribution of cell numbers in FLP-out clones of cells expressing GFP, *Tsc1*, and *Tsc2* (black) or GFP alone (hatched). Mean doubling time (DT) and number of clones counted (n) are indicated.

increase in the population of cells in G1 at the expense of those found in S phase. The proportion of cells in G2 remained unchanged (Figure 4M).

Division times were calculated by generating marked clones of cells and counting the number of cells in the clone after a fixed time interval. Clones that coexpressed *Tsc1* and *Tsc2* were significantly smaller than clones expressing the GFP marker alone (Figures 4O and 4P). This size difference was still observed in the presence of the caspase inhibitor p35, indicating that the reduction in clone size is not due to apoptosis (data not shown). The doubling time of cells that coexpressed *Tsc1* and *Tsc2* was 16.1 hr, which was longer than that of control cells (11.2 hr) (Figure 4Q). Combined with the analysis of the phasing of the cell cycle, these data indicate that all phases of the cell cycle are lengthened in cells that overexpress *Tsc1* and *Tsc2*. However, this effect is most marked for G1, which is lengthened by 75%. The duration of G2 increases by ~47% and the increase in the duration of S phase is only 12%. Thus, a reduction in tissue size can be attributed to a reduction in the size of individual cells as well as a slowing down of cell proliferation.

Tsc1 and *Tsc2* Mutations Interact with G1 Regulators and Increase Cyclin Levels

In the eye disc posterior to the morphogenetic furrow, many cells lacking *Tsc1* displayed elevated levels of Cyclin E, which is localized to the nucleus (Figures 5A–5C), as well as elevated levels of Cyclin A (Figures 5D–5F), which is cytoplasmic. Cells lacking *Tsc2* also have elevated levels of Cyclin A and Cyclin B (Ito and Rubin, 1999).

The size reduction of the eye caused by *Tsc1* and *Tsc2* overexpression was influenced by the expression levels of cyclins that function in the G1 phase of the cell cycle. Overexpression of *cyclin D* and *cdk4* or of *cyclin E* alone using the *eyGAL4* driver did not affect eye size (not shown). However, the phenotype elicited by overexpression of both *Tsc1* and *Tsc2* (Figure 6A) was fully suppressed by the simultaneous overexpression of both *cyclin D* and *cdk4* (Figure 6B) or *cyclin E* (Figure 6D) and partially suppressed by overexpressing *cyclin D* alone (not shown). Conversely, having one mutant allele of either *cdk4*, *cyclin E*, or *cyclin A* enhanced the phenotype (Figures 6C, 6E, and 6F).

Increased activity of insulin-mediated signaling, as well as increased activity of *dmyc* or *Ras1* has been

Table 1. Combined Overexpression of *Tsc1* and *Tsc2* Reduces Cell Size and Cell Number

	Cell densities ($\times 10^{-3}$ cells/μm^2)		Area in compartment ($\times 10^4$ μm^2)		Cell density in posterior compartment (% of control)*	Area of posterior compartment (% of control)*	Cell number in posterior compartment (% of control)*
	Anterior	Posterior	Anterior	Posterior			
control	6.2 (0.2)	5.9 (0.3)	58.4 (2.0)	97.4 (4.5)	100	100	100
UAS-Tsc1	6.3 (0.2)	5.8 (0.3)	54.8 (1.1)	96.7 (2.8)	100	107	107
UAS-Tsc2	6.3 (0.2)	5.8 (0.2)	55.8 (1.2)	96.0 (3.0)	100	105	105
UAS-Tsc1+2	6.5 (0.3)	9.7 (0.7)	54.6 (2.3)	42.7 (3.0)	156	47	73

enGAL4 was used to express *UAS-Tsc1* and *UAS-Tsc2* in the posterior compartment of the wing. Cell densities and compartment size were determined (see Experimental Procedures) and shown as mean values with standard deviations in parentheses (n = 10). Since flies expressing *Tsc1* and *Tsc2* were smaller than wild-type flies, we used the relative sizes of the anterior compartment in wild-type and *UAS-Tsc1*, *UAS-Tsc2* flies to adjust the numbers obtained in the posterior compartment for this effect. Adjusted numbers are indicated in columns marked with an asterisk.

shown to promote growth (reviewed by Stocker and Hafen, 2000). The small eye phenotype induced by overexpression of *Tsc1* and *Tsc2* was suppressed by overexpression of *dmyc* (Figure 6G) and enhanced in flies heterozygous for a mutation in *Ras1* (Figure 6H). Insulin receptor-mediated growth involves activation of the S6 kinase. We found that overexpression of *S6 kinase* suppresses the phenotype induced by overexpression of *Tsc1* and *Tsc2* (Figure 6I). Overexpression of either *dmyc* or *S6 kinase* alone does not affect eye size (not shown). Manipulations that increase the activity of *phosphoinositide 3-kinase (PI3K)*, or that inactivate its antagonist *PTEN*, result in a dramatic increase in cell size (Gao et al., 2000; Goberdhan et al., 1999; Huang et al., 1999; Leevers et al., 1996). Overexpression of *PTEN* alone reduces eye size (Figure 6K). This phenotype enhances that elicited by coexpression of *Tsc1* and *Tsc2* (Figures 6J and 6L). Thus, the phenotype elicited by overexpression of *Tsc1* and *Tsc2* is strongly influenced by the pathways that have been shown to regulate growth in vivo.

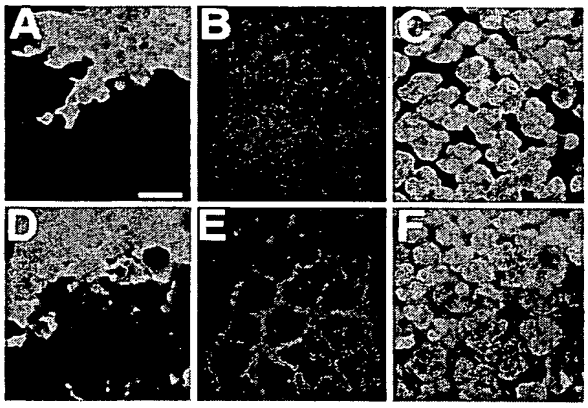

Figure 5. Elevated Levels of Cyclin E and Cyclin A in *Tsc1* Mutant Clones

Third instar eye imaginal discs posterior to the morphogenetic furrow showing photoreceptor cell clusters. Anterior is to the right. Scale bar = 10 μm.

(A and D) Mutant cells fail to stain with anti-β-galactosidase (lilac).

(B) Cyclin E in nuclei is visualized with anti-Cyclin E type 1 (red).

(C) Merge of (A) and (B) with anti-ELAV staining to show photoreceptor nuclei (green). Nuclei that express Cyclin E and ELAV appear yellow.

(E) Cyclin A expression in the cytoplasm visualized with anti-Cyclin A (red).

(F) Merge of (D) and (E) with anti ELAV staining to show exclusion of Cyclin A from photoreceptor cell nuclei (green).

Discussion

Tuberous sclerosis in humans is characterized by the presence of slow growing tumors that often contain giant cells. Here, we present an analysis of the biological properties of the *Drosophila* homologs of *TSC1* and *TSC2*. First, our results show that a mutation in either gene results in large cells that have normal ploidy. Second, we demonstrate that the Tsc1 and Tsc2 proteins function together in vivo. Third, we show that the *Tsc1* and *Tsc2* loci are both important regulators of cell and tissue growth. We also demonstrate that a lack of *Tsc1* or *Tsc2* results in an altered cell cycle characterized by a truncated G1 phase and results in elevated levels of cyclins. Finally, we demonstrate that mutant cells tend to reenter the cell cycle when their wild-type neighbors remain quiescent. This property of mutant cells may be crucial for tumorigenesis in humans.

Tsc1 and *Tsc2* Function Together In Vivo

Mutations in either *Tsc1* or *Tsc2* result in large cells with normal ploidy. The phenotypes of *Tsc1* and *Tsc2* mutants are extremely similar, if not identical. In humans, mutations in either *TSC1* or *TSC2* result in a virtually identical disease. The TSC1 and 2 proteins, hamartin and tuberin, form a complex in cultured cells (Nellist et al., 1999; Plank et al., 1998). Thus, loss of either protein would result in the loss of the complex with the same end result. The disease phenotype in humans and our observations in *Drosophila* suggest that all the functions of TSC1 and TSC2 are mediated by a complex of the two proteins, and that neither protein has additional functions (Figures 2 and 4).

Moreover, combined overexpression of both Tsc1 and Tsc2 readily elicits a phenotype in a variety of tissues, while overexpression of either protein alone is insufficient (Figure 4). This argues that most, if not all, of the endogenous Tsc1 and Tsc2 is sequestered in the complex and is unavailable to complex with exogenously supplied protein.

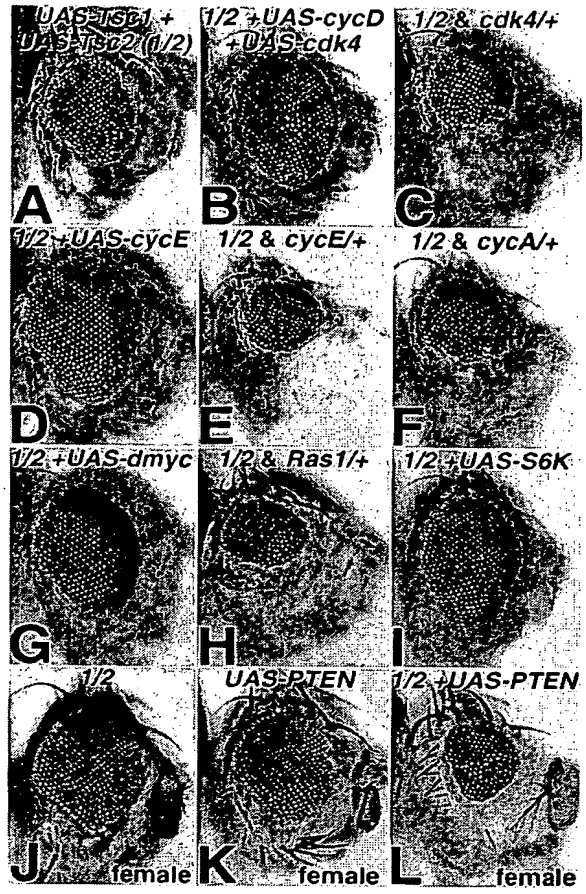

Figure 6. The Phenotype Elicited by Overexpression of *Tsc1* and *Tsc2* Is Modulated by Changes in Levels of Other Regulators of Growth and Cell Proliferation

(A–L) Adult eyes of flies. (A–I) are male and (J–L) are female. Overexpression of *Tsc1* and *Tsc2* under *eyGAL4* control in various genetic backgrounds is abbreviated as "1/2".

Genotypes are: *eyGAL4/+; UAS-Tsc1 UAS-Tsc2/+* (A); *eyGAL4/ UAS-cycD UAS-cdk4; UAS-Tsc1 UAS-Tsc2/+* (B); *eyGAL4/+; UAS-Tsc1 UAS-Tsc2/cdk4*^{3} (C); *eyGAL4/UAS-cycE; UAS-Tsc1 UAS-Tsc2/+* (D); *eyGAL4/ cycE*^{AR95}; *UAS-Tsc1 UAS-Tsc2/+* (E); *eyGAL4/ cycA*^{03946}; *UAS-Tsc1 UAS-Tsc2/+* (F); *eyGAL4/+; UAS-Tsc1 UAS-Tsc2/UAS-dmyc* (G); *eyGAL4/+; UAS-Tsc1 UAS-Tsc2/Ras1*^{e1B} (H); *eyGAL4/UAS-S6K; UAS-Tsc1 UAS-Tsc2/+* (I); *eyGAL4/+; UAS-Tsc1 UAS-Tsc2/+* (female control) (J); *eyGAL4/UAS-PTEN* (K); *eyGAL4/UAS-PTEN; UAS-Tsc1 UAS-Tsc2/+* (L).

Tsc1 and *Tsc2* Regulate Cell and Tissue Growth

Cells mutant for either *Tsc1* or *Tsc2* are larger than wild-type cells and show a marginal decrease in their division time. Thus, the rate of mass accumulation (growth) in *Tsc1* and *Tsc2* mutant cells must be greater than that of wild-type cells to allow them to be larger than their neighbors despite a similar division time. Hence, the primary alteration in the mutants may be an increase in the rate of cellular growth. Conversely, when both *Tsc1* and *Tsc2* are overexpressed, the growth rate of the tissue is reduced (Figure 4). The cells are smaller and take longer to divide than wild-type cells. The increase in duration of the cell cycle may represent an attempt to maintain a near normal cell size in a situation where the rate of growth is reduced. An alternate possibility is that *Tsc1* and *Tsc2* negatively regulate both cell growth and cell cycle progression independently.

The increased growth rate of mutant tissue is apparent in both cycling and postmitotic cells. In cycling populations such as the wing disc and in the eye disc anterior to the morphogenetic furrow, mutant clones are larger than the corresponding wild-type twin spots (Figures 3C and 3F). The difference in size between the clone and the twin-spot becomes more exaggerated after the cells have stopped dividing, resulting in a greatly increased representation of mutant tissue in the adult (Figure 1B).

A major pathway that regulates growth in *Drosophila* is the pathway that links signaling via the insulin receptor to phosphorylation of the ribosomal protein S6. This is thought to lead to increased ribosome biosynthesis and mass accumulation. Thus, loss-of-function mutations in the insulin receptor (*inr*) (Chen et al., 1996), the insulin receptor substrate (*chico*) (Bohni et al., 1999), and in genes encoding the downstream signaling molecules *PI3K* (Weinkove et al., 1999), Akt (*Dakt*) (Verdu et al., 1999), and S6 kinase (*dS6K*) (Montagne et al., 1999), all reduce cell and organ size. Conversely, overexpression of *PI3K* or loss-of-function mutations in the insulin pathway antagonist PTEN (*dPTEN*) lead to increased cell and tissue growth (Gao et al., 2000; Goberdhan et al., 1999; Huang et al., 1999; Weinkove et al., 1999). In addition, *Ras1*, possibly acting via *dmyc*, can also promote cell growth in response to extracellular growth factors (Johnston et al., 1999; Prober and Edgar, 2000). Increased activity of Cyclin D in a complex with cdk4 has also been shown to be a potent stimulus for growth in both dividing and postmitotic cells (Datar et al., 2000).

The enhanced growth observed in the *Tsc1* or *Tsc2* mutants most resembles the results of inactivating *PTEN* (Gao et al., 2000) or increasing *Ras1* or *dmyc* activity (Johnston et al., 1999; Prober and Edgar, 2000). In each of these situations, there is a reduction in the length of the G1 phase. In contrast, increased growth driven by *Cyclin D/cdk4* does not alter the distribution of cells in different phases of the cell cycle (Datar et al., 2000). The effects of the combined overexpression of *Tsc1* and *Tsc2* displays genetic interactions with multiple pathways (Figure 6). The phenotype is influenced by alterations in the levels of *dS6K*, *PTEN*, *Ras1*, *dmyc*, *cyclin D*, and *cdk4*. Thus, *Tsc1* and *Tsc2* may function downstream of the point of convergence of these pathways. Alternatively, *Tsc1* and *Tsc2* may primarily antagonize one of these pathways, but this effect could be overcome by increasing the activity of one of the others.

Imaginal discs containing large mutant clones of either *Tsc1* or *Tsc2* are significantly larger than wild-type imaginal discs but are patterned relatively normally. Mutations in several cell size regulators such as *E2F* or *Rbf* have been shown to affect the size of individual cells but do not alter the final size of the organ (Neufeld et al., 1998). The mechanisms that define organ size are poorly understood. The complex of Tsc1 and Tsc2 restricts the growth of organs in vivo. Screens for genes that interact with *Tsc1* and *Tsc2* are likely to identify additional regulators of organ size.

Tsc1 and *Tsc2* May Modulate the Cell Cycle via Changes in Cyclin Levels

In *Tsc1* and *Tsc2* mutant clones, the levels of both Cyclin E and Cyclin A are elevated (Figure 5). Cell growth driven by *dmyc* or *dTor* elevates Cyclin E levels (Johnston et al., 1999; Oldham et al., 2000; Zhang et al., 2000). It has been postulated that Cyclin E may function as a 'growth sensor' in a manner analogous to CLN3 in yeast (Polymenis and Schmidt, 1997) and that the translation of Cyclin E is more efficient in cells which have an increased rate of growth (Edgar, 1999). The increased levels of Cyclin E may be responsible for the shortening of G1 in *Tsc1* and *Tsc2* mutants. It is unclear why Cyclin A and Cyclin B are also elevated in mutant cells. Cyclin A is normally expressed at high levels in G2. In *Tsc1* or *Tsc2* mutants, Cyclin A levels are elevated in the postmitotic cells of the eye disc which are clearly not arrested in G2. Thus it seems likely that the increased growth in mutant cells may also lead to increased levels of mitotic cyclins. Alternatively Tsc1 and Tsc2 may function in a pathway that negatively regulates cyclin levels.

While the increased levels of cyclins are likely to be a response to the increased growth rate of mutant cells, we cannot exclude the possibility that they are in some way responsible for the increased growth rate. In *Drosophila*, the Cyclin D/cdk4 complex serves to promote growth (Datar et al., 2000). In such a scenario, the loss of *Tsc1* or *Tsc2* gene function may lead to elevated levels of cyclins leading to increased growth and proliferation. Surprisingly, increased expression of Cyclin E, which is thought to primarily promote S-phase entry and not growth, was also able to suppress the phenotype induced by overexpression of *Tsc1* and *Tsc2*. This might reflect the existence of feedback loops where Cyclin E might downregulate the levels or activity of the Tsc1/Tsc2 complex. Alternatively, in some circumstances, Cyclin E might assume some of the functions of the growth promoting Cyclin D. Indeed, in mammalian cells, cyclin E has been shown to fully compensate for the loss of cyclin D1 (Geng et al., 1999).

Tsc1 and *Tsc2* Regulate Cell Cycle Exit

Tsc mutant cells fail to maintain a developmentally induced G1 arrest posterior to the second mitotic wave in third instar eye imaginal discs (Figure 2). The establishment of this G1 arrest requires a downregulation of Cyclin E and Cyclin A expression (Avedisov et al., 2000; Richardson et al., 1995). However, the transient cell cycle arrest in the morphogenetic furrow occurs normally in *Tsc1* and *Tsc2*, suggesting that it is the maintenance of G1 arrest that is perturbed rather than its initial establishment.

Postmitotic cells continue to grow abnormally in *Tsc1* and *Tsc2* mutants and express elevated levels of Cyclin E and Cyclin A. A likely model is that inappropriate and continued growth in postmitotic cells leads to an accumulation of Cyclin E and the mitotic cyclins. This would eventually force cells to overcome a developmentally regulated cell cycle arrest and to reenter the cell cycle. Indeed, many of the lesions in patients with TSC occur in organs that consist predominantly of postmitotic cells such as the heart and brain. A successful therapeutic strategy in tuberous sclerosis is likely to be one that can curtail the inappropriate cell growth.

Experimental Procedures

Fly Stocks

w; FRT82B males were mutagenized with ethylmethanesulfonate (EMS), then crossed to either *y w eyFLP; FRT82B P[mini-w, armLacZ]* or first to *w; TM3/TM6B*, then individually to *y w eyFLP; FRT82B P[mini-w, armLacZ]*. Males with mostly white eyes were retained and maintained as balanced stocks. Alleles of *Tsc1* were *Tsc1*^{087X}, *Tsc1*^{W243X} and *Tsc1*^{R453X}; the allele of *Tsc2*^{192} (formerly *gig*^{192}).

A *Tsc1* cDNA (Ito and Rubin, 1999) was cloned into the pUAST vector using NotI and KpnI sites. A *Tsc2* cDNA was cloned into the NotI site of pUAST. Double (UAS-*Tsc1* and UAS-*Tsc2*) transgenics were generated by recombination between two lines with third chromosome insertions.

Other stocks included *y w eyFLP* (Newsome et al., 2000), *eyGAL4, y w hsFLP; FRT82B P[πMyc] P[w y]* (Xu and Rubin, 1993); *w; FRT80A P[mini-w] P[UbiGFP]/TM6B, w; FRT82B P[mini-w] P[UbiGFP]/TM6B,* and *Act5c>CD2>Gal4 UAS-GFP*$_{NLS}$*S65T (III), UAS-CycD (II), UAS-CycD UAS-Cdk4 (II)* (gifts from L. Johnston and B. Edgar [described in Neufeld et al., 1998; Datar et al., 2000]). *UAS-p35 (II)* was a gift from Bruce Hay. *enGAL4* is described in Neufeld et al., 1998. *cycE*^{P25}, *cycA*^{03946}, *cdk4*^{3}, and *ras1*^{E1B} have been described (Knoblich et al., 1994; Lehner and O'Farrell, 1990; Meyer et al., 2000). *UAS-dPTEN (III)* and *UAS-dmyc (III)* have been described (Gao et al., 2000; Johnston et al., 1999), and *UAS-S6K (II)* was a gift from T. Neufeld.

Microscopy and Immunocytochemistry

Genotypes are described under "Flow Cytometry." Eyes of frozen flies were photographed using a Wild M10 dissecting microscope. Overexpression of *PTEN* + *Tsc1* + *Tsc2* caused lethality in males. Hence, females were used. Wings were mounted in 50% v/v Canada Balsam (Sigma) in methyl salicylate (Fischer); measurements used NIH Image V1.3. Cell densities were assessed by counting the number of wing hairs in a 13,000 μm^2 rectangle at the junction between the wing margin and L2 for the anterior compartment and below the intersection between the posterior cross-vein and L5 for the posterior compartment. The area measured in the anterior compartment was that between the anterior margin and L3 and in the posterior compartment that between L4 and the posterior margin.

Imaginal disc BrdU incorporations were as described (de Nooij and Hariharan, 1995) with a 1.5 hr BrdU pulse to visualize nonsynchronized ectopic S phases posterior to the morphogenetic furrow. The rabbit polyclonal anti-phosH3 antibody was from Upstate Laboratories. The anti Tsc2 antibody is a mouse monclonal antibody 3H1 obtained by immunizing with a fragment containing residues 1203–1531 of the Tsc2 protein and was used at a dilution of 1:5.

Flow Cytometry and Cell Cycle Analysis

Third instar larval wing or eye discs were dissociated and stained as described (Neufeld et al., 1998), run on a Cytomation MoFlo instrument; data were analyzed (including distribution among phases of the cell cycle) using FlowJo (Tree Star Inc.). For loss-of-function analysis, the following genotypes were used: (1) *y w hsFLP/+; FRT82B Tsc1*^{W243X}*/FRT82B P[mini-w] P[UbiGFP]* (2) *y w, hsFLP/+; FRT80A Tsc2*^{192} */FRT80A P[mini-w] P[UbiGFP]*. For gain-of-function analysis, the genotypes were: (1) *y w, hsFLP/+; Act5c>CD2>Gal4, UAS-GFP*$_{NLS}$*S65T (III)/UAS-Tsc1 UAS-Tsc2,* (for overexpression of *Tsc1* and *Tsc2*) (2) *y w hsFLP/+; Act5c>CD2>Gal4, UAS-GFP*$_{NLS}$*S65T (III)/+* (control). Clones were induced at 48 hr after egg deposition (AED) for loss-of-function and 72 hr AED for overexpression, and discs were dissected for analysis at 120 hr AED. Doubling times were calculated as described (Neufeld et al., 1998) using the formula: (log2/logN) × hr. N is the median cell number per clone and hr is the age of the clones in hours. The length of each phase of the cell cycle (in hr) was determined by multiplying the doubling time by the proportion of cells in that phase of the cell cycle.

Cell cycle times in loss-of-function analysis (Figures 3C and 3F) were as follows. Time spent in each phase is in parentheses and time in each phase as percentage of internal control is in square brackets. For discs containing *Tsc1* clones: *control* DT = 14.03 hr (G1 = 4.80 hr; S = 3.61 hr; G2 = 5.63 hr); *Tsc1* DT = 12.76 hr (G1 = 2.45 hr; S = 3.98 hr; G2 = 5.98 hr) [G1 = 51%; S = 110%; G2 = 106%]. For discs containing *Tsc2* clones: *control* DT = 14.88 hr

(G1 = 5.01 hr; S = 3.82 hr; G2 = 5.97 hr); *Tsc2* DT = 13.42 hr (G1 = 2.58 hr; S = 4.36 hr; G2 = 6.79 hr) [G1 = 51%; S = 114%; G2 = 114%]. In the overexpression analysis, (Figure 4Q) time spent in each phase was: *control* (G1 = 3.57 hr; S = 3.75 hr; G2 = 3.84 hr); *Tsc1* + *Tsc2*(G1 = 6.26 hr; S = 4.20 hr; G2 = 5.63 hr).

Acknowledgments

We thank N. Dyson, B. Edgar, M. Frolov, B. Hay, L. Johnston, C. Lehner, T. Neufeld, K. Moberg, O. Stevaux, and K. Tseng for fly stocks; C. Lehner and H. Richardson for antibodies; C. Anniah, S. Jiang, and M. Classon for help with flow cytometry; T. Neufeld, T. Laverty, and G. Rubin for advice and help; S. Mullaney and H. Arruda for injections; S. Schelble and K. Graber for technical assistance; and N. Dyson and S. van den Heuvel for comments on the manuscript. N.T. was funded by an HFSP Long Term Fellowship and I.H. was funded in part by the NIH (EY11632 and GM61672).

Received November 20, 2000; revised April 9, 2001.

References

Avedisov, S.N., Krasnoselskaya, I., Mortin, M., and Thomas, B.J. (2000). Roughex mediates G(1) arrest through a physical association with cyclin A. Mol. Cell. Biol. *20*, 8220–8229.

Bohni, R., Riesgo-Escovar, J., Oldham, S., Brogiolo, W., Stocker, H., Andruss, B.F., Beckingham, K., and Hafen, E. (1999). Autonomous control of cell and organ size by CHICO, a *Drosophila* homolog of vertebrate IRS1–4. Cell *97*, 865–875.

Chen, C., Jack, J., and Garofalo, R.S. (1996). The *Drosophila* insulin receptor is required for normal growth. Endocrinology *137*, 846–856.

Datar, S.A., Jacobs, H.W., de La Cruz, A.F., Lehner, C.F., and Edgar, B.A. (2000). The *Drosophila* cyclin D-cdk4 complex promotes cellular growth. EMBO J. *19*, 4543–4554.

de Nooij, J.C., and Hariharan, I.K. (1995). Uncoupling cell fate determination from patterned cell division in the *Drosophila* eye. Science *270*, 983–985.

Edgar, B.A. (1999). From small flies come big discoveries about size control. Nat. Cell. Biol. *1*, E191–E193.

Ferrus, A., and Garcia-Bellido, A. (1976). Morphogenetic mutants detected in mitotic recombination clones. Nature *260*, 425–426.

Gao, X., Neufeld, T.P., and Pan, D. (2000). *Drosophila* PTEN regulates cell growth and proliferation through PI3K-dependent and -independent pathways. Dev. Biol. *221*, 404–418.

Geng, Y., Whoriskey, W., Park, M.Y., Bronson, R.T., Medema, R.H., Li, T., Weinberg, R.A., and Sicinski, P. (1999). Rescue of cyclin D1 deficiency by knock in cyclin E. Cell *97*, 767–777.

Goberdhan, D.C., Paricio, N., Goodman, E.C., Mlodzik, M., and Wilson, C. (1999). *Drosophila* tumor suppressor PTEN controls cell size and number by antagonizing the Chico/PI3-kinase signaling pathway. Genes Dev. *13*, 3244–3258.

Gomez, M.R. (1988). Tuberous Sclerosis, Second Edition. (New York: Raven Press).

Hendzel, M.J., Wei, Y., Mancini, M.A., Van Hooser, A., Ranalli, T., Brinkley, B.R., Bazett-Jones, D.P., and Allis, C.D. (1997). Mitosis-specific phosphorylation of histone H3 initiates primarily within pericentromeric heterochromatin during G2 and spreads in an ordered fashion coincident with mitotic chromosome condensation. Chromosoma *106*, 348–360.

Henry, K.W., Yuan, X., Koszewski, N.J., Onda, H., Kwiatkowski, D.J., and Noonan, D.J. (1998). Tuberous sclerosis gene 2 product modulates transcription mediated by steroid hormone receptor family members. J. Biol. Chem. *273*, 20535–20539.

Huang, H., Potter, C.J., Tao, W., Li, D.M., Brogiolo, W., Hafen, E., Sun, H., and Xu, T. (1999). PTEN affects cell size, cell proliferation and apoptosis during *Drosophila* eye development. Development *126*, 5365–5372.

Ito, N., and Rubin, G.M. (1999). *gigas*, a *Drosophila* homolog of tuberous sclerosis gene product-2, regulates the cell cycle. Cell *96*, 529–539. Erratum: Cell *105*, this issue, 415.

Johnston, L.A., Prober, D.A., Edgar, B.A., Eisenman, R.N., and Gallant, P. (1999). *Drosophila* myc regulates cellular growth during development. Cell *98*, 779–790.

Knoblich, J.A., Sauer, K., Jones, L., Richardson, H., Saint, R., and Lehner, C.F. (1994). Cyclin E controls S phase progression and its down-regulation during *Drosophila* embryogenesis is required for the arrest of cell proliferation. Cell *77*, 107–120.

Kobayashi, T., Hirayama, Y., Kobayashi, E., Kubo, Y., and Hino, O. (1995). A germline insertion in the tuberous sclerosis (Tsc2) gene gives rise to the Eker rat model of dominantly inherited cancer. Nat. Genet. *9*, 70–74.

Kobayashi, T., Minowa, O., Kuno, J., Mitani, H., Hino, O., and Noda, T. (1999). Renal carcinogenesis, hepatic hemangiomatosis, and embryonic lethality caused by a germ-line Tsc2 mutation in mice. Cancer Res. *59*, 1206–1211.

Lamb, R.F., Roy, C., Diefenbach, T.J., Vinters, H.V., Johnson, M.W., Jay, D.G., and Hall, A. (2000). The TSC1 tumour suppressor hamartin regulates cell adhesion through ERM proteins and the GTPase Rho. Nat. Cell. Biol. *2*, 281–287.

Leevers, S.J., Weinkove, D., MacDougall, L.K., Hafen, E., and Waterfield, M.D. (1996). The *Drosophila* phosphoinositide 3-kinase Dp110 promotes cell growth. EMBO J. *15*, 6584–6594.

Lehner, C.F., and O'Farrell, P.H. (1990). The roles of *Drosophila* cyclins A and B in mitotic control. Cell *61*, 535–547.

Meyer, C.A., Jacobs, H.W., Datar, S.A., Du, W., Edgar, B.A., and Lehner, C.F. (2000). *Drosophila* cdk4 is required for normal growth and is dispensable for cell cycle progression. EMBO J *19*, 4533–4542.

Miloloza, A., Rosner, M., Nellist, M., Halley, D., Bernaschek, G., and Hengstschlager, M. (2000). The TSC1 gene product, hamartin, negatively regulates cell proliferation. Hum. Mol. Genet. *9*, 1721–1727.

Montagne, J., Stewart, M.J., Stocker, H., Hafen, E., Kozma, S.C., and Thomas, G. (1999). *Drosophila* S6 kinase: a regulator of cell size. Science *285*, 2126–2129.

Nellist, M., van Slegtenhorst, M.A., Goedbloed, M., van den Ouweland, A.M., Halley, D.J., and van der Sluijs, P. (1999). Characterization of the cytosolic tuberin-hamartin complex. Tuberin is a cytosolic chaperone for hamartin. J. Biol. Chem. *274*, 35647–35652.

Neufeld, T.P., de la Cruz, A.F., Johnston, L.A., and Edgar, B.A. (1998). Coordination of growth and cell division in the *Drosophila* wing. Cell *93*, 1183–1193.

Newsome, T.P., Asling, B., and Dickson, B.J. (2000). Analysis of *Drosophila* photoreceptor axon guidance in eye-specific mosaics. Development *127*, 851–860.

Oldham, S., Montagne, J., Radimerski, T., Thomas, G., and Hafen, E. (2000). Genetic and biochemical characterization of dTOR, the *Drosophila* homolog of the target of rapamycin. Genes Dev. *14*, 2689–2694.

Onda, H., Lueck, A., Marks, P.W., Warren, H.B., and Kwiatkowski, D.J. (1999). Tsc2(+/−) mice develop tumors in multiple sites that express gelsolin and are influenced by genetic background. J. Clin. Invest. *104*, 687–695.

Plank, T.L., Yeung, R.S., and Henske, E.P. (1998). Hamartin, the product of the tuberous sclerosis 1 (TSC1) gene, interacts with tuberin and appears to be localized to cytoplasmic vesicles. Cancer Res. *58*, 4766–4770.

Polymenis, M., and Schmidt, E.V. (1997). Coupling of cell division to cell growth by translational control of the G1 cyclin CLN3 in yeast. Genes Dev. *11*, 2522–2531.

Prober, D.A., and Edgar, B.A. (2000). Ras1 promotes cellular growth in the *Drosophila* wing. Cell *100*, 435–446.

Richardson, H., O'Keefe, L.V., Marty, T., and Saint, R. (1995). Ectopic cyclin E expression induces premature entry into S phase and disrupts pattern formation in the *Drosophila* eye imaginal disc. Development *121*, 3371–3379.

Robinow, S., and White, K. (1991). Characterization and spatial distribution of the ELAV protein during *Drosophila melanogaster* development. J. Neurobiol. *22*, 443–461.

Soucek, T., Pusch, O., Wienecke, R., DeClue, J.E., and Hengstschlager, M. (1997). Role of the tuberous sclerosis gene-2 product in cell cycle control. Loss of the tuberous sclerosis gene-2 induces quiescent cells to enter S phase. J. Biol. Chem. *272*, 29301–29308.

Stocker, H., and Hafen, E. (2000). Genetic control of cell size. Curr. Opin. Genet. Dev. *10*, 529–535.

Tsuchiya, H., Orimoto, K., Kobayashi, K., and Hino, O. (1996). Presence of potent transcriptional activation domains in the predisposing tuberous sclerosis (Tsc2) gene product of the Eker rat model. Cancer Res. *56*, 429–433.

Verdu, J., Buratovich, M.A., Wilder, E.L., and Birnbaum, M.J. (1999). Cell-autonomous regulation of cell and organ growth in *Drosophila* by Akt/PKB. Nat. Cell. Biol. *1*, 500–506.

Weinkove, D., Neufeld, T., Twardzik, T., Waterfield, M., and Leevers, S. (1999). Regulation of imaginal disc cell size, cell number and organ size by *Drosophila* class I (A) phosphoinositide 3-kinase and its adaptor. Curr. Biol. *9*, 1019–1029.

Wienecke, R., Konig, A., and DeClue, J.E. (1995). Identification of tuberin, the tuberous sclerosis-2 product. Tuberin possesses specific Rap1GAP activity. J. Biol. Chem. *270*, 16409–16414.

Xiao, G.H., Shoarinejad, F., Jin, F., Golemis, E.A., and Yeung, R.S. (1997). The tuberous sclerosis 2 gene product, tuberin, functions as a Rab5 GTPase activating protein (GAP) in modulating endocytosis. J. Biol. Chem. *272*, 6097–6100.

Xu, T., and Rubin, G.M. (1993). Analysis of genetic mosaics in developing and adult *Drosophila* tissues. Development *117*, 1223–1237.

Yeung, R.S., Xiao, G.H., Jin, F., Lee, W.C., Testa, J.R., and Knudson, A.G. (1994). Predisposition to renal carcinoma in the Eker rat is determined by germ-line mutation of the tuberous sclerosis 2 (TSC2) gene. Proc. Natl. Acad. Sci. USA *91*, 11413–11416.

Young, J., and Povey, S. (1998). The genetic basis of tuberous sclerosis. Mol. Med. Today *4*, 313–319.

Zhang, H., Stallock, J.P., Ng, J.C., Reinhard, C., and Neufeld, T.P. (2000). Regulation of cellular growth by the *Drosophila* target of rapamycin dTOR. Genes Dev. *14*, 2712–2724.